

FULL PAPER

Quantitative insights into the Fast Pyrolysis of Extracted Cellulose, Hemicelluloses and Lignin

Marion Carrier,^{*[a]} Michael Windt,^[b] Bernhard Ziegler,^[b] Jörn Appelt,^[b] Bodo Saake^[c], Dietrich Meier^[b] and Anthony Bridgwater^[a]

Abstract: The transformation of lignocellulosic biomass into bio-based commodity chemicals is technically possible. Among thermochemical processes, fast pyrolysis, a relatively mature technology that has now reached the commercial level, produces a high yield of an organic-rich liquid stream. Despite the recent efforts in elucidating the degradation paths of biomass pyrolysis, the selectivity and recovery rates of bio-compounds remain low. In an attempt to clarify the general degradation scheme of biomass fast pyrolysis and provide a quantitative insight, this study has combined the use of fast pyrolysis micro-reactors, spectrometric techniques (i.e. mass spectrometry and nuclear magnetic resonance) and mixtures of unlabelled and Carbon-13 enriched materials. The first stage of the work reported aimed at selecting the type of reactor to ensure control of the pyrolysis regime. The comparison of chemical fragmentation patterns of 'primary' fast pyrolysis volatiles detectable by GC-MS between two small scale micro-reactors has shown the inevitable presence of secondary reactions. In a second stage, liquid fractions also made of 'primary' fast pyrolysis condensables have been analysed by quantitative liquid-state ¹³C-NMR providing a quantitative distribution of functional groups. The compilation of those results into a map that displays the distribution of functional groups according to the individual and main constituents of biomass (e.i. hemicelluloses, cellulose, and lignin) confirmed the origin of individual chemicals within fast pyrolysis liquids.

Introduction

Fast pyrolysis of plant biomass has now reached the technological and commercial maturity to convert solid materials into bio-oil^[1]. Expected formerly to provide a solution for the replacement of fossil-based liquid products, these bio-oils are more recently seen as potential feedstock for chemicals from an integrated biorefinery perspective^[2]. However, a number of concerns regarding the quality of fast pyrolysis bio-oil have been raised (i.e., instability, high variability in chemical composition, high water content, immiscibility with petroleum-derived fuels, changing viscosity, phase separation) preventing its upgrading for any commercial applications.^[3] In particular, the high level of oxygen within fast-pyrolysis oils requires the application of

intensive post-treatments to selectively deoxygenate these liquids; resulting in the intense scientific activity in the field of catalytic fast pyrolysis^[4] and bio-oil upgrading in the last decade.^[5] A considerable number of catalysts has been developed as a result of the chemical diversity of the components in bio-oils.^[4] Whatever the processing approach used (i.e. ex-situ or in-situ) or catalysis approach (i.e., homogeneous or heterogeneous), it is reasonable to think that a better understanding of the origin of the constituent chemicals in bio-oil could have a beneficial impact on the overall performance of these processes.

The understanding of biomass pyrolysis mechanisms creates a real challenge when considering the large diversity of type of biomass and fast pyrolysis technologies. For several decades, a number of researchers have tried to elucidate the main degradation pathways for biomass fast pyrolysis modelling.^[6-11] As a result, the overall degradation scheme of biomass fast pyrolysis is seen as an interplay between physical and chemical events, which are often impossible to separate.^[12] Evans and Milne have described a degradation scheme pointing out the main degradation pathways according to process conditions with by-products classified as primary, secondary and tertiary^[9]. More recently, researchers have questioned the nature of the proposed mechanisms. Indeed, the chemical aspect of biomass fast pyrolysis can be described as a combination of parallel and successive reactions of non-ionic and ionic nature^[13]. If radical mechanisms are often invoked and are predominant in coal pyrolysis^[14], recent experimental evidences^[6,7,15] and theoretical calculations^{[16][17]} for biomass fast pyrolysis suggest the predominance of non-ionic reactions during the primary pyrolysis stage. This on-going discussion on the importance and predominance of the ionic and/or non-ionic character of fast pyrolysis reactions^[13] has provided important clues that have not yet been used to rationalize the degradation modes. This is mainly due to a lack of rigorous analytical methodology and the absence of control of reaction regimes that leads to contradictory interpretations of mechanisms. For example, the control of heating rate is of importance when discussing types of mechanisms, as the heating rates selected have a direct influence on the chemical composition of the bio-oil. Experimental evidence has shown a significant change in the quality of bio-oil when using slow or fast pyrolysis^[18].

In addition to being process-dependent, the chemical composition of bio-oil is also affected by the nature of the lignocellulose feed material. In an attempt to identify and delineate the chemical reactions related to the transformation of individual biopolymers (i.e. cellulose, hemicelluloses and lignin), researchers have opted for the use of model compounds and different analytical strategies. Most of the degradation pathways that have been suggested until now are based on the thermal degradation of model compounds, which leads to oversimplified degradation schemes and a biased picture of the composition of bio-oil. However, these studies have been instrumental in revealing key

- [a] Dr., M., Carrier, Prof. Anthony Bridgwater
European Bioenergy Research Institute
Aston University Birmingham B4 7ET, UK
E-mail: m.carrier@aston.ac.uk
- [b] M. Windt, B. Ziegler, Dr. J. Appelt, Prof. D. Meier
Thünen Institute of Wood Research
Bio-based Resources and Materials
Leuschnerstr. 91, 21031 Hamburg
- [c] Prof. B. Saake, University of Hamburg, Chemical Wood
Technology, Leuschnerstr 91, 21031 Hamburg
Supporting information for this article is given via a link at the end of the document.

FULL PAPER

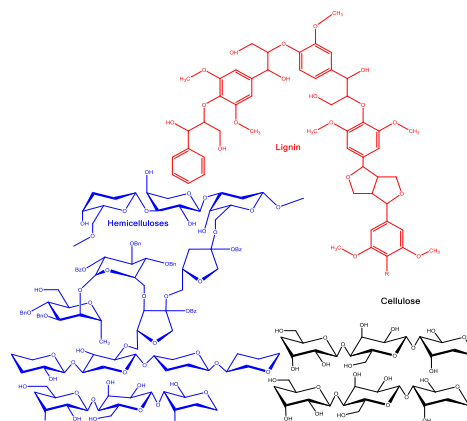
patterns. Indeed several pathways and fast pyrolysis mechanisms have been reported for the production of valuable chemicals [19][20]. Despite significant progress over the last 30 years, a fundamental understanding of fast pyrolysis chemistry, i.e. the key mechanistic details leading to the formation of fast-pyrolysis bio-oil, is still lacking for a number of reasons: (i) the identification of chemical reactions based on the conversion of model compounds often leads to oversimplified degradation schemes; (ii) the inability of analytical techniques to immediately, fully and unequivocally describe bio-oil; and finally (iii) control of the pyrolysis regime is often impractical. When studying degradation patterns, we cannot avoid mentioning isotopic spectrometric techniques. Indeed, the use of non-radioactive isotopes as tracers have been instrumental in providing further details on fragmentation mechanisms by allowing the distinction between intramolecular and intermolecular reactions, the quantitative assessment of the conversion of specific individual carbon atoms (i.e. carbon-13) in a molecule into other products, to mention a few examples.

To bring forward the current knowledge on the primary mechanisms of biomass 'fast' pyrolysis, we propose to follow an analytical procedure to assess and quantify the levels of 'primary' products under controlled 'fast' conditions. Carbon-13 enriched materials in conjunction with spectrometric techniques are used to provide a more representative and quantitative description of bio-oils. This study confirms and clarifies general degradation scheme for biomass fast pyrolysis by providing a quantitative insight.

Results and Discussion

Characterization of raw materials

¹³C labelled and unlabelled leaves from natural *Zea Mays* grown under controlled conditions are composed of cellulose, hemicelluloses and lignin evenly distributed, with 30-38 wt.% of Glucan, 23-25 wt% of Xylan and 20-26 wt% of Klason lignin [21]. The main blocks were extracted following classical methods. Cellulosic and hemicellulosic fractions were obtained using the classical method of a two-step sulphur-free soda pulping with sodium boron hydride in the first step to protect soluble hemicelluloses [22] followed by further purification through selective bleaching and extraction steps allowing the separation of cellulose from hemicelluloses. Lignin was isolated from the black liquor obtained by two-step sulphur-free soda pulping adopted in a slightly modified form from Nadji *et al.* [23]. Based on the sugar composition (Supporting information TS1) and details of extraction techniques (more details provided in Supporting information FS1), a representation of the lignocellulosic composition of *Zea Mays* is proposed (Scheme 1). It is interesting to note the broad chemical composition of the hemicelluloses which contain between 55-62% of xylose, 22-25% arabinose and 8-9% of galactose; agrees with previous results [21][24].



Scheme 1. Potential illustration of lignocellulosic blocks extracted from *Zea Mays*.

The extracted biopolymers displayed a low degree of purity, of between 58-59 % for cellulose, 48-50% for hemicelluloses and 40-47 % for lignins; all fractions containing different levels of impurities. For example, in the hemicellulosic fraction, 2.1-7.8 wt% of glucose remains with some lignin fragments and inorganics. The cellulosic fraction contains a substantial amount of xylan at 22.9 wt%. For the technical lignin, it is established that a significant fraction of sugars remain within the material as not all linkages of the lignin-carbohydrate complex are broken [25] with sugars levels reaching up to 3.2 wt. % [26].

With respect to the presence of inorganics, a semi-quantification of major elements using SEM/EDS analysis revealed the ash composition within raw and technical materials (Supporting information TS2). The inorganic fraction of cellulose is mainly composed of Si, while Na and Ca make up that of hemicelluloses and Si and Na that of lignin. If the presence of some of these inorganic elements can be explained by the natural composition of the original plant, e.g. *Zea Mays*, for which the inorganic matter is mostly composed of K and Ca, high levels of Na in both hemicelluloses and lignin could originate from salts contained in solutions or solvents used to extract or precipitate technical materials.[27]

Ultimate analysis of individual materials (Table 1) have allowed the deduction of general elemental formulae (Table 2). Their comparison with literature indicates the chemistry of the technical biopolymers differs from that of native constituents due the presence of residual components. The chemical extraction had a substantial impact on the chemical composition of the lignin that sees its chemical structure significantly altered. Indeed, during the acid precipitated process of soda lignins, phenolic hydroxyls are lost and condensation reactions are favoured with the formation of carboxyl groups.[26]

FULL PAPER

Table 1. Ultimate analysis of unlabelled and extracted materials in (wt.%).

Feedstock	C	H	N	S	O+Ash	H/C
Maize	41.6	5.65	1.31	0.06	51.4	0.14
Cellulose	42.8	6.38	0	0	50.9	0.15
Hemicelluloses	34.6	5.35	0.75	0	59.3	0.16
Lignin	49.9	6.08	1.43	0	42.6	0.12

Table 2. General chemical formula.

	Cellulose	Hemicelluloses	Lignin
This study	C _{5.6} H ₁₀ O ₅	C ₅ H ₉ O _{6.5}	C ₈ H ₁₁ O ₅
Literature Measured		C _{5.2} H _{9.7} O ₅ ^[28]	C _{10.2} H _{12.2} O _{3.8} N _{0.2} ^[7]
General	(C ₆ H ₁₀ O ₅) _n ^[29]	(C ₅ H ₈ O ₄) _n and (C ₆ H ₁₀ O ₅) _n ^[30]	

Identification of pyrolysis products by Py-GC/MS technique

The detection (Figure 1) and identification of organics by Py-GC/MS (Figure S2) proved to be useful in revealing some clear thermal and structural differences between technical biopolymers.

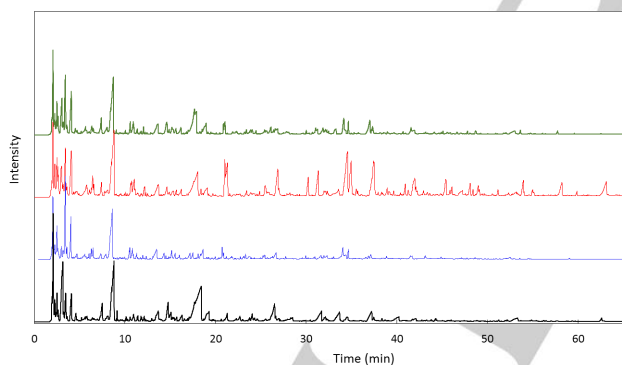


Figure 1. Chromatogram (GC-FID) resulting from the pyrolysis of extracted biopolymers from *Zea Mays*: (—) mixture; (—) cellulose; (—) hemicelluloses and (—) lignin.

The detection of some typical components confirmed the botanical origin of the material, *Zea Mays*, as a grass. For example, the detection of ribofuranoside, pyranoses and furanoses compounds (Supplementary data, TS 3) confirms the highly heterogeneous nature of hemicelluloses in grasses has an arabinoxylan structure^[31]. For lignin, the detection of aromatic components: phenols (e.g. phenol, 2-methyl, phenol, 4-dimethyl, phenol, 4-ethyl); guaiacols (e.g. 4-methylguaiacol (creosol), 4-ethylguaiacol, p-vinylguaiacol) and syringols (e.g. phenol, 2,6-

dimethoxy-4,2-propenyl) (ST 3) confirms the presence of p-hydroxyphenyl (H), guaiacyl (G), and syringyl (S) phenylpropanoid units within the original material. As expected, a number of sugars (e.g. 1,4: 3,6-dianhydro- glucopyranose) were detected in the technical lignin; confirming the intimate bonding between carbohydrates and lignin and the difficulty in separating them chemically.

Within a molecular range between 25-300 Da, the number of chemicals detected and identified is low. Indeed, the detection capability of gas chromatographic techniques are limited to the volatility of products and the heaviest compounds such as oligomers are not analysed. To solve this technical issue, alternative chromatographic conditions (e.g. a change of columns) or techniques (e.g. GPC) must be used^[7]. In this study, we exploit the performance of liquid-state nuclear magnetic resonance (NMR) to assess the chemical composition of the whole bio-oil but this is certainly less specific in terms of organics identification but certainly more representative of its chemical composition.

Nature of primary reactions

There is no a unanimous consensus when naming and listing the number of degradation stages, which is the direct consequence of the complex character of fast pyrolysis; but researchers tend to agree that the thermal degradation of lignocellulose occurs through a series of primary, secondary and tertiary multiphase chemical reactions and are transformed into stable organic vapours and aerosols, carbonaceous residue and permanent gases^[32].

The overall degradation scheme of biomass 'fast' pyrolysis can be seen as a combination of parallel and competing reactions, whose occurrence and dominance is feedstock and process-related. The pyrolysis regime obeys the thermodynamic laws of transport (mode) and transfer (limitations), mainly controlled by the design of the reactor and the feedstock's preparation. Researchers have mapped the different pyrolysis regimes according to characteristic times (Figure 2). The use of these characteristic times that illustrate the predominance of times between internal conduction to the external convection (thermal Biot number, Biot nb), between chemical reaction and internal conduction (Internal pyrolysis number, Py') or external convection (Darcy number, Da or external pyrolysis number, Py'') have permitted the boundaries to be defined. As a result, the pyrolysis regime must be controlled to allow the deduction of biomass degradation patterns in real-world reactors and under 'fast' conditions.

FULL PAPER

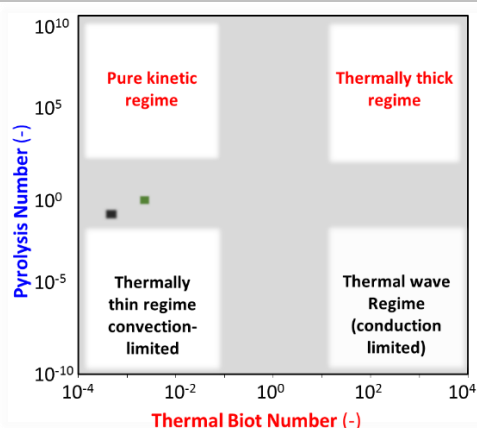
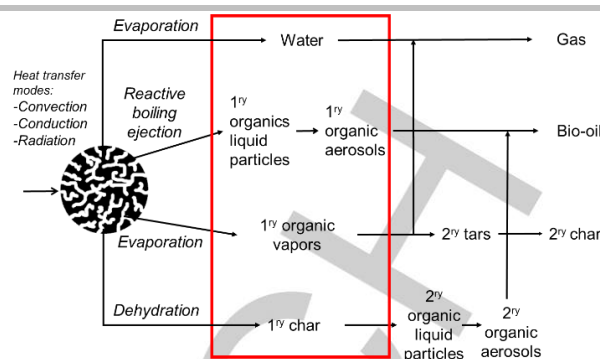


Figure 2. Mapping of pyrolysis regimes according to heat transport. Adapted from Paulsen *et al.* [33]. Heat-transport map for (■) Pyroprobe; (■) Micro-reactor at ca. 550°C.

In this study, two fixed bed reactors with distinct designs have been used to transform technical biopolymers. The non-dimensional numbers, Biot and Pyrolysis numbers, have been estimated, which have permitted actual pyrolysis modes to be specified within experiments for the same characteristic length of the biomass particles. The values corresponding to internal heat transport number, Py , and thermal Biot number results have been placed in the heat-transport map (Figure 2). Pyrolysis is not isothermal in both Pyroprobe and micro-reactor and heat transport differs by one order of magnitude with the obvious occurrence of heat and mass transfer limitations. This result is not surprising when we see the major advancements that have been made recently in the development of experimental micro-reactors to address temperature gradient [33] and temporal mismatch [34] interfering with the kinetics of reactions. When it comes to studying primary reactions, it is important to prevent or limit the occurrence of any secondary reactions. In general, solid particles and volatiles that spend a short residence time (< 1 s) in the hot zone are classified as 'primary products' and result mainly from fragmentation and shrinkage of particles. These primary products have different physical states: aerosols, vapours and/or gas for volatiles and solids. When they are retained in the hot zone, volatiles and residual solid undergo secondary reactions resulting in the formation of secondary products (Scheme 2). These secondary reactions are typically categorized as heterogeneous gas-solid reactions and homogeneous gas-phase reactions. The heterogeneous reactions include intra- and inter-particle reactions between solid (unconverted biomass and/or char) and gas or liquid and gas, which result in secondary char and low molecular weight volatiles [35].



Scheme 2. Intra- and extra-particle mass and heat transport events.

Although it has been demonstrated that it would be impossible to prevent any intra-particle secondary reactions, it is however technically possible to control the number of extra-particle secondary reactions by limiting the volatile residence time within the hot-zone.

To assess the impact of extra-particle residence time of volatiles on chemical reactions, an isotopic labelling approach using non-radioactive materials and mass spectrometry technique was used. Fragment recombinations between primary volatiles species and more specifically the modes of initial carbon-carbon bond-breakage within the biopolymers could thus be studied [36]. Detailed analyses of MS fragmentation patterns for furfural (See Supplementary data Figures S2 & S3, Tables S4 & S5), produced through primary reactions [37], from the pyrolysis of mixtures between unlabelled and ^{13}C enriched materials using Py-GC/MS and the micro-reactor are respectively shown in Figures 3a, 3b and 3c. In the case of the mixed cellulose and lignin preparation processed through Py-GC/MS, the good match between experimental fragmentation and predicted patterns confirms the absence of carbon scrambling during the primary fast pyrolysis stage; indicating the dominance and the unimolecular character of intramolecular rearrangements. When processing the three-biopolymer mixture, the difference between calculated and experimental values became more noticeable (Figure 3b). This could result in less predictable conversion due to the increasing complexity of reactions when adding hemicelluloses.

Discrepancies between experimental and calculated values became even more prominent when the 3-biopolymer mixture was processed in the micro-reactor as shown in Figure 3c. The use of the tubular micro-reactor with a longer volatile residence of 1.8 s (vs the order of milliseconds for the pyroprobe) had an adverse impact with the presence of secondary reactions. That is best represented by comparing the distribution ratios for $m/z = 95$ and $m/z = 96$ (Figures 3a, 3b and 3c), where Furfural production is significantly decreased when volatiles are exposed to longer residence times in the hot zone. Overall, the results suggest that the presence of chemical interactions when hemicelluloses is added and the volatiles residence time was extended affect chemistry of primary reactions.

FULL PAPER

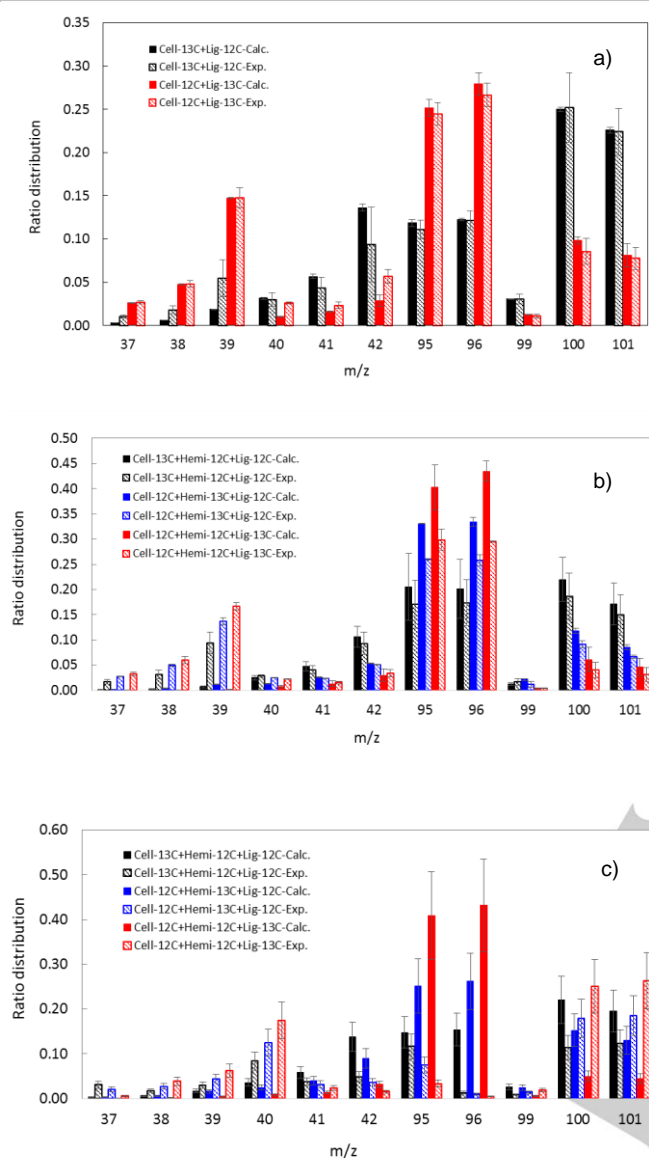


Figure 3. Confirmation of the product identity, furfural, and lack of scrambling by comparing experimental and predicted MS fragmentation patterns (Ratio distribution vs mass/charge ratio- m/z) of FP products from mixtures of unlabelled cellulose (Cell-12C), hemicelluloses (Hemi-12C) lignin (Lig-12C) and carbon-13 enriched cellulose (Cell-13C), hemicelluloses (Hemi-13C) and lignin (Lig-13C) – a) Mixtures of Cellulose and Lignin processed in Py-GC/MS; b) and c) Mixtures of Cellulose, Hemicelluloses and Lignin processed respectively in Py-GC/MS and the micro-reactor.

Micropyrolysis of extracted biopolymers and their mixtures

Each extracted biopolymer and their mixtures were fast pyrolyzed at 550°C using a conventional tubular reactor (Figure S4). As expected, the extracted cellulose displayed the lowest char yield (Figure 4). The solid residue is often attributed to the formation of 'primary char' resulting from the dehydration and charring processes of solid polymers and to the formation of 'secondary char', which result from polymerization reactions between volatile

compounds.^[35] This latter is maximized when volatiles are exposed to extensive heterogeneous residence times (i.e. solid-volatiles residence time)^[38]. During the pyrolysis process, the volatiles were continuously and immediately removed from the hot zone at 550°C and were only exposed to a homogeneous residence time (i.e. volatiles residence time) less than 1.8 s. Fast pyrolysis of lignin led to ca. 28.4 wt.% char yield in the range of those obtained from the conversion of raw biomass and mixtures, 26.1 and 27.0 wt.%. Although the presence of lignin has been reported to be the origin of char^[39], its transformation led to lower char yields than those resulting from the conversion of hemicelluloses (Figure 4). The result can be explained by the presence of sugar impurities that may have inhibited the formation of char facilitating the devolatilization of lignin, but also by the aromatic character and heterogeneous nature of hemicelluloses used in this study.

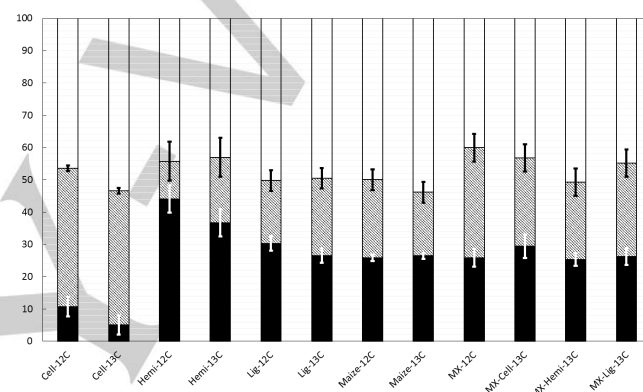


Figure 4. Yield of fast pyrolysis products for 550°C. (■) char yield; (■ + □) volatiles yield; (□) total GC-detectable product yield; (□) non-detected products yield obtained by difference.

Product distribution according GC/MS analysis

A portion of the fast-pyrolysis bio-oil could be analysed using an off-line GC-MS technique. In total, 142 pyrolysis products have been identified and 55 quantified (TS6). These compounds have been lumped by chemical families according different classifications. A preliminary classification, grouping these organics according their non-aromatic, heterocyclic and aromatic character (Figure S5), indicates that most of the products detected by GC-MS (non-aromatic and carbohydrates) have a non-aromatic character.

Refined degradation patterns can be obtained by adopting a detailed classification of organic compounds as presented in Figure 5. The concentration of detected products differs according the nature of the biopolymer processed. Highest levels, up to 40 wt.%, were detected by GC for cellulose, which dropped to 16 and 21 wt.% for hemicelluloses and lignin, respectively. The carbohydrates character of cellulose-derived bio-oil was confirmed with the detection of 20.75 wt.% sugars. The highest level of acids (8.56 wt.%) was found for the hemicelluloses-derived bio-oils; indicating that the hemicellulosic fraction of biomass should be at the origin of the acidic character of bio-oils, and uronic acid groups present in hemicelluloses^[30] Equivalent

FULL PAPER

amounts of acids and sugars, 3.87 and 4.91 wt.%, within lignin-derived liquids confirm the less acidic character than that of hemicellulosic liquids. In particular, the high levels of short acids (e.g. acetic and propionic acids levels of 4.8 and 3.8 wt.% detected for hemicelluloses-derived liquids against 1.8 and 2.1 wt. % for the lignin-derived liquids) have been found to have a catalytic effect on the oligomerization of phenolic compounds. This has been experimentally demonstrated in the presence of acetic acid [7], while the role of propionic acid still remains unknown. It is noteworthy that only the lignin-derived liquids displayed a monomeric phenol fraction that derived from the hydroxyl and methoxy-substituted phenylpropane units [40].

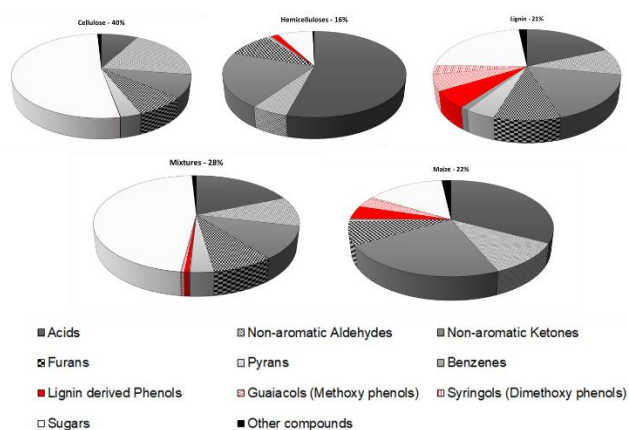


Figure 5. Relative proportions (%) of the important fractions in bio-oil.

Cellulose degradation patterns

Despite the vast number of cellulose degradation schemes available, a common pattern is reported and can be summarized as follows: (i) depolymerization of cellulose into glucose through transglycosylation/retro-aldol condensation (intramolecular rearrangement of the monomeric units); (ii) β -elimination with the production of levoglucosan, which is further degraded into hydroxyacetaldehyde via (iii) ring fragmentation.^[41]

The detection of high concentrations of levoglucosan (LG, 20.85 wt.%) and hydroxyacetaldehyde (HA, 5.32 wt.%) confirms the preponderance of the β -elimination mechanism in cellulose deconstruction under fast pyrolysis. The level of LG remains much lower than that recorded when the reactor design allows the preservation of molten-phase for longer times^[15]; confirming that the selectivity towards LG can be increased by minimizing homogeneous secondary reactions and increasing the heat flux density. This loss in LG selectivity was beneficial to the formation of other anhydrosugars (e.g. Anhydro- β -D-arabinofuranose, 1,5-; Anhydro- β -D-xylofuranose, 1,5-; Anhydro- α -D-galactofuranose, 1,6-; Dianhydro- α -D-glucopyranose, 1,4:3,6-) with an average of 20.8 wt.%; thus indicating that secondary pyrolysis is abundant in this conventional tubular micro-reactor.

But also high levels of smaller products such as furans (e.g. 2.83 wt.% HMF-5 and 0.94 wt.% furfural) and small oxygenates (e.g. 1.13 wt.% acetic acid and 1.47 wt.% propionic acid) indicate that ring fragmentation of cellulose leads directly to the large portion of furanic products^[37]; and that this degradation pathway (iii) is

favoured over elimination reactions leading to pyrans (e.g. 1.23 wt.% of Pyran-4-one, 3-hydroxy-5,6-dihydro-, (4H)-) and anhydrosugars.

Hemicelluloses degradation patterns

The main degradation events for the pyrolysis of hemicelluloses in general the least investigated among major lignocellulosic blocks can be summarized as follows: (i) depolymerisation of the xylan fraction into xylose via the breakdown of the glycosidic bond, (ii) production of anhydrosugars and pyran compounds via rearrangement, (iii) competing reactions between the ring breakage of the anhydrosugars and pyrans into light oxygenates (e.g., carboxylic acids, aldehydes and furans containing between one and five carbons).

When considering the GC-MS analyses, the selection of pure standards based on major degradation of cellulose and lignin did not permit the main degradation trends to be described and represented only 16 wt.% of organics within the condensates (Figure 5). The high levels of acetic, propionic acids and hydroxypropanone, (4.8, 3.8 and 0.9-3.3 wt.%, are still an indication that the hemicellulosic fraction contains a number of ring units that are easily breakable into light oxygenates and that the acetyl groups that are usually sensitive to alkaline hot extraction^[42] have been retained in the structure. In the list of identified compounds, a number of 5 carbons heterocyclics not detected in the case of cellulose and lignin strongly support the idea that thermal processing of hemicellulosic fraction may result in a new range of chemicals. The transformation of these technical hemicelluloses did not lead to LG; indicating that the cellulosic fraction, 2.1-7.8 wt.% (TS 1), that is left after extraction could have little impact on the final product distribution.

When compared to previous work on fast pyrolysis of extracted hemicelluloses^[6], considerable deviations with the composition of condensates were observed. This is mainly attributed to the different botanical origin of the feedstock from which the hemicelluloses were extracted. Indeed, *Zea Mays leaves*-derived hemicelluloses contained less xylose, 31.1-31.6 wt.% on average (TS1), compared to levels occurring in switchgrass, 66.2 wt.%^[6]. We may also expect that the type of isolation and/or purification methods also influenced this product distribution. The most obvious difference was the detection of propionic acid instead of formic acid from *Zea Mays*. The disparity between yields and nature of carboxylic acids was attributed to the different heat transfer and reaction time scales used by both studies, a heating rate of 452°C/s in our case vs the claimed rapid heating rate of > 2000 °C/s^[37]. Faster heating rates promoting the rupture of the –H₂C-COOH linkage.

Among the levels detected, the carboxylic acids with an average amount of 8.6 wt.% are the most abundant followed by 3.4 wt.% of non-aromatic ketones, 1.4 wt.% of furans, 1.2 wt.% of sugars and 0.87 wt.% of non-aromatic aldehydes. Substantial amounts of ketones and furans have also been detected when converting extracted hemicelluloses in a tubular fixed-bed reactor^[43,44]; the furfural being also the most abundant furanic compound. The highest concentrations of acetic acid detected confirmed that hemicelluloses remain the biopolymer that produces most of this acid.

Lignin degradation patterns

FULL PAPER

When fast pyrolyzed, lignin is converted into both unstable and stable products through two competitive reactions: (i) thermal cleavage of inter-unit or alkyl linkages and (ii) char formation. The primary condensates are mainly composed of monomeric phenolic compounds^[7]. This was confirmed by the detection of a range of phenols (e.g. 0.18 wt.% of phenol, 0.60 wt.% of phenol, 4-vinyl), methoxy- (e.g. 0.17 wt.% of guaiacol, 0.52 wt.% of guaiacol, 4-vinyl, 0.14 wt.% of vanillin) and dimethoxy- phenols (e.g. 0.17 wt.% of syringol, 0.13 wt.% of syringol, 4-vinyl and 0.14 wt.% of acetosyringol). In this study, the relative ratio of phenols (P), guaiacols (G) and syringols (S) units was P:G:S 1.1:1.0:0.6, when compared to the original ¹³C enriched *Zea Mays*, of 2.1:1.0:0.9. This was determined by approximating the ¹³C liquid-state CP/MAS spectrum^[21], which indicated that a large proportion of monolignol units was not fully released. This confirms the liberation of oligomers, most probably dimers^[7] containing 2 phenols units connected by a 5-5 biphenyl type linkage, which is the most recalcitrant towards thermal cleavage^[45].

In addition to phenylpropane units of various degrees of methoxylation, the lignin fraction of the native *Zea mays* possesses numerous side chains with different types of carbons C α , C β , C γ and oxygenated groups such as alcohol, carbonyl and carboxylic acid functions^[21]. When pyrolyzed, these side chains generate light oxygenates carboxylic acids (e.g. 1.8 wt.% of acetic acid, 2.1 wt.% of propionic acid).

Degradation patterns of raw biomass and mixtures of three biopolymers

The distribution of major pyrolysis products from *Zea mays* corresponds to that depicted for each biopolymer; that is high levels of light oxygenates (7.0 wt.% of carboxylic acids, 2.5 wt.% of non-aromatic aldehydes and 4.1 wt.% of non-aromatic ketones in bio-oil produced), a common trend for all lignocellulosic fractions. A quasi similar product distribution in light oxygenates was obtained for the mixture (5.1 wt.% of carboxylic acids, 2.8 wt.% of non-aromatic aldehydes and 3.0 wt.% of non-aromatic ketones in bio-oil). Some furans and pyrans, 1.7 wt.% and 0.13 wt.% respectively, were also produced and are attributed to the degradation of cellulose. Only a few lignin-derived compounds (e.g. phenol, 4-vinyl and guaiacol, 4-vinyl) were detected at a total concentration of 1.0 wt.% and derived from technical hemicelluloses and lignin transformations. This low production of lignin-derived products, 0.2 wt.%, was also measured when both hemicelluloses, cellulose and lignin were mixed and converted.

A striking difference in the product distribution is the level of sugars produced, 3.2 wt.% for the native biomass against 13.5 wt.% for mixtures.

Another distinctive feature between conversion of biomass and mixtures of technical biopolymers is the level of hydroquinone, 3.1 wt.%, which has been detected at a really low level for the mixture, 0.1 wt.%, and yet it appears to be a common compound detected on many occasions when studying the pyrolysis of biomass^{[9][46]} and technical lignin^[47]. Also there was an unexpected low level of levoglucosan, 0.6 wt.% for the biomass vs 10.4 wt.% on average for mixtures. Finally, the thermal conversion of mixtures produced a low amount of lignin-derived compounds, 0.2 wt.% vs 1.0 wt.% for biomass.

The mixture ratio between C, H and L was based on compositional analyses of the same feedstock, *Zea Mays*, found in the literature that indicates that the hemicellulosic fraction makes up the largest part of the feedstock. Although we cannot therefore guarantee the perfect reproduction of the lignocellulosic composition of the native material, the comparison of product yields between the raw biomass and mixture confirms the key role of linkages and additives (i.e. extractives and inorganics) during pyrolysis. The association of those components prevents the efficient release of monolignols and greatly affects the degradation patterns of cellulose. For instance, the formation of hydroquinone combined with changes in the pyrolysis degradation patterns of all biopolymers is an indicator that the presence of a 'radical scavenger' character^[48], such as hydroquinone, could interfere and reassign the dominance of fast pyrolysis degradation modes (i.e. ionic and non-ionic modes).

When considering the yields of individual key products for bio-oils derived from mixtures, the production of cellulose-derived products (e.g. glycoaldehyde, levoglucosan, 5-HMF) was not enhanced and that of lignin-derived products substantially suppressed. These results indicate that the reported beneficial effect of the presence of lignin on cellulose degradation and vice-versa during primary pyrolysis^[35] was inhibited by the presence of hemicelluloses. These results indicate that the mechanistic explanation suggested by Hosoya *et al.*^[35]: 'polymerization of anhydrosugars is inhibited by the lignin-derived volatile products' to the benefit of oxygenated 5C heterocycles production is unlikely to happen under those fast pyrolysis conditions. However these results confirmed the competition between the cleavage of glycosidic and C-C bonds, which has now been reported many times^[35].

Quantitative liquid-state ¹³C-NMR analysis

Until very recently liquid NMR techniques became widely used in the field of biomass pyrolysis product analysis as these methods provide a more accurate view of the chemical composition of condensates by mapping the overall distribution of functional groups. This reveals important changes in the chemistry of pyrolysis according to pyrolysis regimes in terms of non-dimensional characteristic numbers^[18]. However considering both the small amount of condensables that can be collected under controlled 'fast' pyrolysis and the low natural abundance of the ¹³C isotope, the use of ¹³C enriched substrates has permitted their analysis by increasing the magnitude of NMR resonance signals (Figure S6)^[21].

Since the extracted biopolymers used in this study have low purity we noticed further resonance lines derived from the impurities (e.g. the presence of xylans in the cellulose-derived condensates, glucan in hemicellulosic-based liquids and sugars in the liquid produced from impure technical lignin) during the NMR analyses.^[49] This has been taken into consideration when attributing the relevant chemical shift regions to the corresponding chemical functions (Figure S6) according to chemical shift ranges proposed by previous studies (See Table 3 in Experimental part).

The relative distribution of functional groups within bio-oil as determined by quantitative liquid ¹³C-NMR (Figure 6 and Table S7), indicates that methoxy or hydroxyl carbons prevail in cellulose- and mixture-derived ¹³C-enriched liquids; confirming

FULL PAPER

that a large proportion of aliphatic C-O functions within condensates is related to the carbohydrate fraction in biomass. Secondary alkyl carbons represent the largest proportion in lignin-derived condensates, due to the highly branched character of the polyphenolic structure with side chains containing secondary carbons^[27]. The large amount of aliphatic C-C bonds combined with the lack of carbon scrambling confirms that this type of linkage was not cleaved during the primary 'fast' pyrolysis reactions and refuting any mechanistic suggestions that proposed the participation of these groups in the formation of aromatics. A significant amount of these secondary carbons was also found in hemicellulose-derived liquids; a tempting interpretation would be to suggest hemicelluloses as a potential source of long carbon chains. The overall chemical composition of bio-oils produced from the fast pyrolysis of raw *Zea Mays* was found to best match that of lignin-derived liquids (TS 8); suggesting that the chemical composition of volatiles generated during fast pyrolysis of lignocellulose is significantly affected by the presence of the polyphenolic biopolymers.

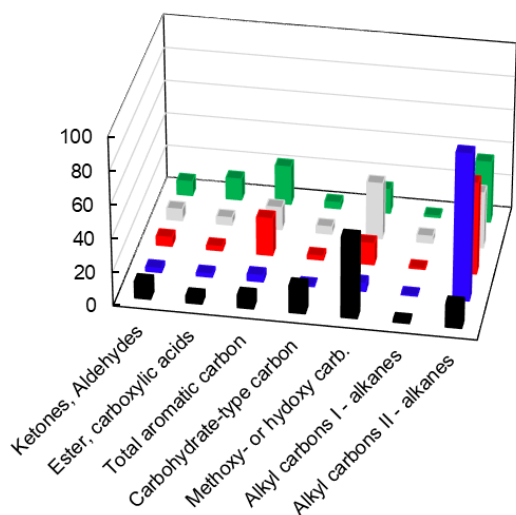


Figure 6. Relative portion (%) of chemical groups within enriched bio-oils based on liquid-state ^{13}C NMR analyses: (■) Cell- ^{13}C ; (■) Hemi- ^{13}C ; (■) Lig- ^{13}C ; (■) MX- ^{13}C ; (■) Maize- ^{13}C .

Carbon source issue from fast pyrolysis reactions.

To confirm the origin of functional groups according to the lignocellulosic composition, the co-pyrolysis of one ^{13}C enriched polymer mixed with two unlabeled polymers was performed.

Using the quantitative results from liquid-state ^{13}C NMR analysis, it was also possible to determine the origins of the carbon by carefully distinguishing between contributions from ^{13}C NMR signals from ^{13}C enriched and unlabeled materials. More detailed information can be found in Supplementary Data.

Figure 7 shows most of the carbohydrate's products and shows that functional groups such as methoxy/hydroxyl carbons and alkyl primary carbons are mostly derived from cellulose.

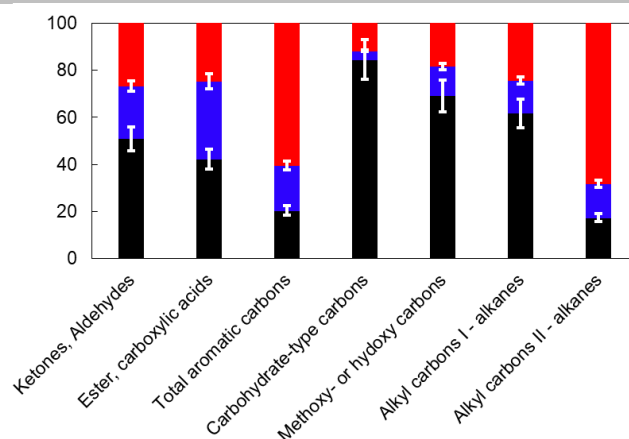


Figure 7. Carbon source for chemical families according extracted biopolymers: (■) Cellulose; (■) Hemicelluloses; (■) Lignin.

Ratio deviations (Figure 8) were calculated from experimental and estimated values of ^{13}C moles per gram of condensates. The values were obtained from the experimental results for each technical component pyrolysis weighted by their mass percentage proportion within mixtures assuming that there is no interaction between these biopolymers. The difference between the experimental and estimated yields (i.e., deviation from the X-axis in Figure 8) provides the extent of these interactions. Most significant deviations were obtained for cellulose-derived products with substantially lower intensity for carbohydrates-type carbons and methoxy or hydroxyl carbons implying that the degradation pattern of cellulose is greatly affected by the presence of hemicelluloses and lignin. This result confirms the important role of cellulose-hemicelluloses and cellulose-lignin bonding respectively ascribed to hydrogen^[50] and ether^[51] bonding. On the contrary, the degradation patterns of hemicelluloses and lignin remained consistent, the ratio deviation varied in a small range. In some cases, the detection of some chemical families (i.e. alkanes containing primary alkyl carbons) tend to slightly increase in the presence of cellulose.

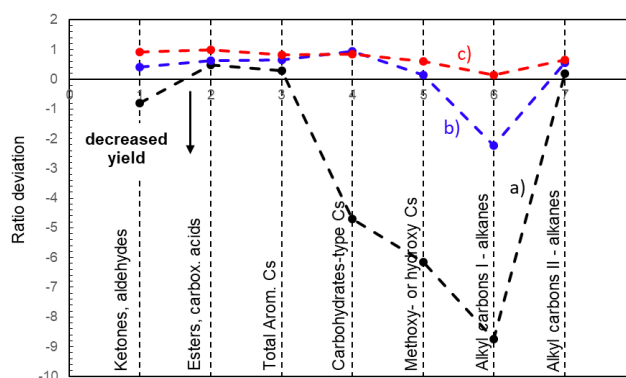


Figure 8. Ratio deviation between experimental and theoretical yields of organic groups for: a) Cellulose; b) Hemicelluloses and c) Lignin.

Conclusions

FULL PAPER

Fast pyrolysis of technical cellulose, hemicelluloses, lignin and their mixtures was compared in an attempt to provide a more explicit thermal degradation scheme for lignocellulosic material. The conversion of these biopolymers was achieved by means of two different fast pyrolysis micro-reactors (i.e. pyroprobe and tubular micro-reactor) set at 550°C. The use of isotopic spectrometric techniques was also explored to provide a quantitative view of the overall product distribution under fast pyrolysis conditions.

Combining the fast pyrolysis product distributions obtained from extracted unlabelled and carbon-13 enriched cellulose, hemicelluloses and lignin, the current results permit a degradation model to be developed for biomass fast pyrolysis where products have been lumped according to the original lignocellulosic distribution of biomass. This novel NMR spectrometric approach which combines the overall analysis of bio-oil by ¹³C-NMR and isotopically labelled starting materials will certainly be increasingly useful to express global kinetic expressions.

The comparison of degradation patterns between native biomass and mixtures of extracted lignocellulosic biopolymers indicates a potential 'inhibitor' role of catechols driving degradation modes.

Liquid carbon-13 nuclear magnetic resonance in association with the use of Carbon-13 enriched isotopic material has permitted the technical limitations to be overcome related to the low natural abundance of ¹³C (1.1 %); thus making the interpretation of ¹³C NMR spectra much easier and more reliable. The applicability of our approach to the widespread pyrolysis conditions needs to be tested. If successful, the use of labelled compounds combined with ¹³C-NMR should become a useful tool for assessing the stoichiometry of balanced chemical equations.

Experimental Section

Cellulose and hemicelluloses extraction

Zea Mays was subjected to a series of extractions (i.e. 1st cold ethanol extraction (0-4 °C) followed by a Soxhlet ethanol/toluene (2:1, v/v) followed by hot water extraction at 100°C before further extractions.

Cellulose and hemicelluloses were extracted following the classical two-step sulphur-free soda pulping method proposed by Huisman et al. [22]. The 1st step consisted in the pre-treatment of the washed biomass using a 10% NaOH solution (10% on dry matter basis at a solid-liquid ratio 1:10 at 60°C for 1 h) in the presence of a sodium boron hydride solution. The cellulosic solid was bleached by hydrogen peroxide (5% H₂O₂), extracted with diluted (2%) alkali, again bleached by hydrogen peroxide (5% H₂O₂), washed and vacuum-dried (at 40°C). Its purity (after hydrolysis) was analyzed by HPLC (Dionex HPAEC-PAD).

The hemicellulosic fraction was obtained by precipitation of supernatants from the 1st pre-hydrolysis step using ethanol, followed by an acid hydrolysis and a last selective precipitation of the glucoronarabinoxylans with water.

Lignin extraction

The isolation of alkali-solv Lignin, more commonly named Soda lignin was done according to a two-step sulphur-free soda pulping method established by Nadji et al. [23] with some modifications. The pulping stage consisted in subjecting a mixture of *Zea Mays*:liquor (Na₂O) 4:1 (w/w) at ca. 120°C for 1.5 h. The lignin was precipitated from the black liquor with concentrated formic acid, to pH 3, and cooled overnight to 4 °C. The resulting precipitate (lignin) was isolated by centrifugation, washed twice with 10% formic acid, and three times with demineralized water to pH 5-6, followed by freeze-drying.

Feedstocks characterization and preparation

Raw unlabelled and ¹³C enriched *Zea Mays* leaves (Maize-¹²C & Maize-¹³C) as well as unlabelled and ¹³C enriched cellulose (Cell-¹²C & Cell-¹³C), hemicelluloses (Hemi-¹²C & Hemi-¹³C) and lignin (Lig-¹²C & Lig-¹³C) extracted from *Zea mays* leaves were purchased from IsoLife (Wageningen, The Netherlands). The unlabelled feedstocks all displayed a natural abundance in ¹³C less than 1.3 atom% while all labelled materials were uniformly enriched with ¹³C content above 97 atom%. Elemental analysis of individual feedstocks was performed using a Flash 2000 Organic Elemental Analyzer (Thermo Fisher Scientific) and the sulphaniamide as standard (CE Instrument).

Particle size distribution was determined from SEM images. – Particle size: 50-150 µm.

Analysis of inorganic elements: Samples (i.e., raw materials and chars) were analysed with a Philips XL30 FEG ESEM scanning microscope combined with an Oxford Instruments INCAx EDS. A standard analysis protocol was applied. Samples were deposited onto the double-sided adhesive carbon mounting tabs and carbon coated using an Emscope SC500 sputter coater. These analyses were utilised to provide particle size distribution, topographical and morphological images of particles and to semi-quantify the composition of major inorganic elements.

Preparation of feedstocks for Py-GC/MS: Mixtures of Cell-¹²C+Lig-¹²C, Cell-¹³C+Lig-¹²C and Cell-¹²C+Lig-¹³C were prepared according to a mass ratio of 7:3 using a Sartorius microbalance (Model ME36S). This ratio was selected according to a previous study that applied Technical Association of the Pulp and Paper Industry (TAPPI) standard methods (T264 om-88, T211 om-85) for determining the compositional analysis of corn stover with proportions (i.e. holocellulose, cellulose and lignin) determined gravimetrically. The lignocellulosic composition given was about 42.3 wt.% of hemicelluloses (determined by difference), 37.0 wt.% of cellulose and 13.0 wt.% of lignin.[52] The mixtures prepared from extracted materials were mixed for 4h using a roller mixer (Model SRT6D) at a speed of 60 rpm.

Preparation of feedstocks for the micro fast pyrolyzer: Raw unlabelled and enriched *Zea Mays* leaves were cryo milled in a cryogenic freezer/mill (Spec SamplePrep Model 6750) for 2 mins/cycle. A cooling time of 15 min was set between the 2 milling cycles to avoid any overheating of the biomass.

Mixtures of Cell-¹²C+Hemi-¹²C+Lig-¹³C, Cell-¹³C+Hemi-¹²C+Lig-¹²C, Cell-¹²C+Hemi-¹³C+Lig-¹²C and Cell-¹²C+Hemi-¹²C+Lig-¹³C were prepared according to a mass ratio of 4:4.5:1.5 using a Sartorius microbalance (Model ME36S) and roller mixed for 24 hours before use.

Pyrolyzer-GC-MS/FID

Fast pyrolysis of individual components and mixtures were performed with a CDS 5200 pyroprobe (CDS Analytical). The reactor consisted of an open quartz tube (25 mm length, 1.9 mm ID) that was inserted inside a heated probe. The quartz tube was electrically heated with a platinum coil which was calibrated according to the supplier specifications. The feedstock was placed into the open quartz tube (CDS Analytical) on the top of a quartz wool bed (CDS Analytical). A gas flow of Helium (Pure Helium, 99.996%, BOC) of 18 mL/min was maintained to continuously remove the volatiles from the hot zone. Before being analysed, the volatiles passed through different isothermal zones: (i) the on-line/off-line valve oven permitting the heating and cooling of the interface zone, (ii) a trapping zone (Tenax-TA™ pre-column (PerkinElmer) set at 310°C) preventing any secondary reactions between volatiles of happening and (iii) a heated transfer line (CDS Analytical) set at 310°C) connected on the chromatographic system.

For each experiment, a small amount of material, between 0.6 and 2 mg (Sartorius microbalance - ME36S model), was introduced into the quartz tube and subjected to a heating rate of 452°C/s to reach the desired pyrolysis temperature of 550°C for 1.5 s. These conditions were selected to mimic the time-temperature history of a particle within a bubbling

FULL PAPER

fluidized bed reactor^[53]. On-line analysis of volatiles was done via a PerkinElmer GC-MS/FID system (Clarus 680-Clarus 600S). Their separation was done by using an Elite 1701 column (30 m*0.25 mm*0.25 μm film thickness). Helium was used as carrier gas set at 15 mL min⁻¹. The sample was injected at 275°C using a split ratio of 1:50. The heating program of the oven was programmed as followed: starting heating from 45°C to 280°C at a rate of 2.5 °C/min. Once separated, the organics were identified using a mass to charge ration of 30-300 Da. The MS spectra obtained were compared to the standard spectra of compounds found in the NIST library (2011). The identity of each compound was confirmed only if the fragmentation pattern with the detection of major m/z signals and intensity distribution matched the NIST spectrum. The order of separation was checked to according the retention time of pure standards found in a previous study using the same system^[54].

Micro fast pyrolysis and volatiles condensation

The horizontal system consists of a quartz tube (length: 50 cm and internal diameter: 1 cm heated by two independent horizontal furnaces. Both heated zones were controlled by two independent thermocouples placed between the outer surface of the quartz tube and the heating element. The quartz boat that holds the feedstock (ca. 20 mg) is placed in the first zone of the tube at room temperature before the two heated zones. Once the boat is placed and both furnace pre-heated at the desired temperature, the tube is flushed with pure Nitrogen (Linde 5.0) set at a flow rate of 50 mL/min (ADM2000 Agilent flowmeter) under atmospheric pressure. The boat is introduced into the first heated zone using a magnetic manipulator. Fast pyrolysis takes place at a fixed temperature of 550°C and the sample is maintained in the zone for 70 s. After this required time, the boat is moved rapidly to its initial position. Volatiles (i.e. vapours and aerosols) pass through the second heated element set at 350°C; to prevent them to condensing on the tube's wall before their collection. Condensable volatiles were immediately quenched by using a vapour trapping system (i.e., a pear shaped flask made of borosilicate glass with glass cold finger), which is placed in a beaker containing dry ice and acetone at around -50°C. The permanent gases were allowed to exit through a cotton wool filter. Once the condensables are collected, the trapping system is disconnected and sealed before further analyses. The boat is removed and weighted using a Mettler Toledo XSE205 microbalance. All different parts of the setup were cleaned thoroughly with water/acetone and dried at 105°C. Char yield is directly calculated, while volatiles yield is determined by difference. Reproducibility of yields was achieved by pyrolyzing *Pinus Radiata* wood three times for which a standard deviation of 2.3 wt.% for char yield was obtained.

Condensates characterization by GC-MS/FID

Once the beaker reached room temperature, the film of condensables deposited on the walls was recovered using 500 μL of an acetone solution containing 209.48 μL/mL of fluoranthene (Sigma-Aldrich, 99%) as an internal standard and an additional 100 μL of acetone (Sigma-Aldrich, ≥ 99.9%). The identification and quantification of condensables was performed with a HP 6890 Agilent gas chromatography system coupled to a HP 5972 mass spectrometer. The GC was equipped with a Varian VF 1701-MS column (14%-cyanopropylphenyl – methylpolysiloxane, 60 m x 0.25 mm dimension; 0.25 μm film thickness). The carrier gas used was helium (Linde) at an initial flow rate of 1.3 mL/min and 225.7 kPa constant pressure. The injection was operated at 250°C in a split mode (50:1) with a split flow of 66.1 mL/min and a total flow of 70.2 mL/min. A second wash was applied to ensure the complete recovery of condensates with 100 μL of acetone containing 2.263 mg/mL of internal standard (IS) and 1000 μL of pure acetone. This last sample was injected in a split less mode. The GC column was initially heated at 45°C for 4 min and then from 45 to 280°C at 3°C/min and held for 20 min. The quantification of compounds was done via FID operating at 280°C using a hydrogen flow rate of 40.0 mL/min and an air flow rate of 450.0 mL/min. The detection was done using MS operated in the scan acquisition mode (19-550 amu). The MS source and MS quadruple temperatures were 230 °C and 150 °C, respectively. The identification and quantification of compounds was performed with the software OpenChrome using a home-made library elaborated at VTI-Institute of Wood Technology. The quantification of 55 compounds was done based on calibration curves. Reproducibility of the GC-detectable content measurements was assessed by injecting three times the collected volatiles resulting in standard deviation of 0.2 and 0.3 wt.% for the 1st and 2nd wash, respectively.

Quantitative ¹³C-NMR

Liquid-state ¹³C-NMR analyses were performed with a Bruker Avance 3 400 MHz for 1H NMR spectroscopy system. DMSO-*d*₆ (99.8 %, deuterium) was used as solvent and Hexamethyldisiloxane (> 98 %, Aldrich) as internal standard. The condensates (~15-20 mg) were directly collected from the glassware by adding 600 μL of an internal standard solution, whose composition depended on the type of feedstock processed. For non-labelled bio-oil samples, a volume of 600 μL internal standard solution HMDSO:DMSO-*d*₆ = 1:250 (w:w) was used. For enriched bio-oil sample, a solution of HMDSO:DMSO-*d*₆ = 1:30 (w:w). NMR spectra were acquired using inverse-gated decoupling pulse sequences, 90° pulse angle, with a relaxation delay of 5.5 s (5*T₁=D₁) between pulses. In order to maintain a reasonable analysis time a relaxation agent, 2.1 mg of Chromium-acetylacetonate (Cr(acac)₃) (Sigma-Aldrich, 99.99%) was added to every NMR sample. The resulting experiments, however, still required several hours to obtain sufficient signal-to-noise that allowed for the integration of spectra. Considering the operating conditions and the good repeatability for GC/MS analysis done on fast pyrolysis condensates of controlled and ¹³C enriched materials, no duplication of ¹³C NMR measurement was performed. However, the accuracy of NMR analysis was determined by integrating the signal on a spectral width of 1 ppm in the frequency domain where no signal was detected for each spectrum.

Table 3. Chemical shifts ranges for ¹³C-NMR.

Chemical range (ppm)	shift	Groups	Reference
215-180		Ketones, aldehydes	[55]
180-163		Esters, carboxylic acids	[55]
163-110:		Aromatic (general):	[56], [57]
• 125-112		Aromatic compounds (guaiaacyl compounds)	
• 112-110		Aromatic compounds (syringyl compounds)	
110-84		Carbohydrate type carbons	
84-54		Methoxy, hydroxyl bond compounds (R- <u>C</u> H ₂ -O-R, R-O- <u>C</u> H ₃)	
54-1:		Primary, secondary, tertiary & quaternary alkyl carbons	
• 34-24		Most of secondary & tertiary alkyl carbons	
• 24-6		Most of primary & some secondary alkyl carbons	

Acknowledgements

The authors acknowledge the European Union and Horizon 2020 to financially support the action H2020-MSCA-IF-2014, Pyrochem Grant 656967, entitled: "Biopolymers ¹³C Tracking during Fast Pyrolysis of Biomass - A 2-Level Mechanistic Investigation". Technical support from Ingrid Fortman and Bernhard Ziegler (VTI-Institute of Wood Technology and Wood Biology, Hamburg, Germany) for respectively undertaking the compounds quantification from GC-MS and carrying out the NMR analyses is gratefully acknowledged. And finally, the authors would like to thank Dr. Khalid Doudin for providing valuable advices for the treatment of NMR spectra.

Keywords: fast pyrolysis • primary reactional mechanisms • technical biopolymers • biomass • spectrometry

FULL PAPER

- [1] D. Meier, B. Van De Beld, A. V. Bridgwater, D. C. Elliott, A. Oasmaa, F. Preto, *Renew. Sustain. Energy Rev.* **2013**, *20*, 619–641.
- [2] S. K. Maity, *Renew. Sustain. Energy Rev.* **2015**, *43*, 1446–1466.
- [3] a. V. Bridgwater, *Chem. Eng. J.* **2003**, *91*, 87–102.
- [4] C. Liu, H. Wang, A. M. Karim, J. Sun, Y. Wang, *Chem. Soc. Rev.* **2014**, *43*, 7594–7623.
- [5] C.-H. Zhou, X. Xia, C.-X. Lin, D.-S. Tong, J. Beltramini, *Chem. Soc. Rev.* **2011**, *40*, 5588–617.
- [6] P. R. Patwardhan, R. C. Brown, B. H. Shanks, *ChemSusChem* **2011**, *4*, 636–643.
- [7] P. R. Patwardhan, R. C. Brown, B. H. Shanks, *ChemSusChem* **2011**, *4*, 1629–1636.
- [8] J. Svenson, J. B. C. Pettersson, K. O. Davidsson, *Combust. Sci. Technol.* **2004**, *176*, 977–990.
- [9] R. J. Evans, T. a Milne, *Energy & Fuels* **1987**, *1*, 123–138.
- [10] C. Di Blasi, G. Signorelli, C. Di Russo, G. Rea, *Ind. Eng. Chem. Res.* **1999**, *38*, 2216–2224.
- [11] C. Branca, P. Giudicianni, C. Di Blasi, *Ind. Eng. Chem. Res.* **2003**, *42*, 3190–3202.
- [12] C. Di Blasi, *Chem. Eng. Sci.* **1996**, *51*, 1121–1132.
- [13] V. Mamleev, S. Bourbigot, M. Le Bras, J. Yvon, *J. Anal. Appl. Pyrolysis* **2009**, *84*, 1–17.
- [14] M. L. Poutsma, *J. Anal. Appl. Pyrolysis* **2000**, *54*, 5–35.
- [15] M. S. Mettler, A. D. Paulsen, D. G. Vlachos, P. J. Dauenhauer, *Energy Environ. Sci.* **2012**, *5*, 7864.
- [16] V. Seshadri, P. R. Westmoreland, *J. Phys. Chem. A* **2012**, *116*, 11997–12013.
- [17] H. B. Mayes, L. J. Broadbelt, *J. Phys. Chem. A* **2012**, *116*, 7098–7106.
- [18] H. Ben, A. J. Ragauskas, *Bioresour. Technol.* **2013**, *147*, 577–584.
- [19] J. V Ortega, A. M. Renehan, M. W. Liberatore, A. M. Herring, *J. Anal. Appl. Pyrolysis* **2011**, *91*, 190–198.
- [20] M. M. Ramirez-Corredores, *Pathways and Mechanisms of Fast Pyrolysis*, © 2013 Elsevier B.V. All Rights Reserved., **2013**.
- [21] M. Foston, R. Samuel, A. J. Ragauskas, *Analyst* **2012**, *137*, 3904.
- [22] M. M. H. Huisman, H. A. Schols, A. G. J. Voragen, *Carbohydr. Polym.* **2000**, *43*, 269–279.
- [23] H. Nadji, P. N. Diouf, A. Benaboura, Y. Bedard, B. Riedl, T. Stevanovic, *Bioresour. Technol.* **2009**, *100*, 3585–3592.
- [24] B. C. Saha, R. J. Bothast, *Appl. Biochem. Biotechnol.* **1999**, *76*, 65–77.
- [25] A. Tejado, C. Peña, J. Labidi, J. M. Echeverria, I. Mondragon, *Bioresour. Technol.* **2007**, *98*, 1655–1663.
- [26] R. J. A. Gosselink, A. Abächerli, H. Semke, R. Malherbe, P. Käuper, A. Nadif, J. E. G. Van Dam, *Ind. Crops Prod.* **2004**, *19*, 271–281.
- [27] S. Constant, H. L. J. Wienk, A. E. Frissen, P. de Peinder, R. Boelens, D. S. van Es, R. J. H. Grisel, B. M. Weckhuysen, W. J. J. Huijgen, R. J. A. Gosselink, et al., *Green Chem.* **2016**, *18*, 2651–2665.
- [28] S. Wang, B. Ru, G. Dai, W. Sun, K. Qiu, J. Zhou, *Bioresour. Technol.* **2015**, *190*, 211–218.
- [29] C. Liu, R. Sun, in *Thermochem. Convers. Biomass to Liq. Fuels Chem.*, **2010**, pp. 131–167.
- [30] J. Ren, R. Sun, in *Thermochem. Convers. Biomass to Liq. Fuels Chem.*, **2010**, pp. 73–130.
- [31] M. Pauly, K. Keegstra, *Plant J.* **2008**, *54*, 559–568.
- [32] A. R. Teixeira, K. G. Mooney, J. S. Kruger, C. L. Williams, W. J. Suszynski, L. D. Schmidt, D. P. Schmidt, P. J. Dauenhauer, *Energy Environ. Sci.* **2011**, *4*, 4306.
- [33] A. D. Paulsen, M. S. Mettler, P. J. Dauenhauer, **2013**.
- [34] C. Krumm, J. Pfaendtner, P. J. Dauenhauer, *Chem. Mater.* **2016**, *28*, 3108–3114.
- [35] T. Hosoya, H. Kawamoto, S. Saka, *J. Anal. Appl. Pyrolysis* **2007**, *80*, 118–125.
- [36] J. B. Paine, Y. B. Pithawalla, J. D. Naworal, C. E. Thomas, *J. Anal. Appl. Pyrolysis* **2007**, *80*, 297–311.
- [37] M. S. Mettler, S. H. Mushrif, A. D. Paulsen, A. D. Javadekar, D. G. Vlachos, P. J. Dauenhauer, *Energy Environ. Sci.* **2012**, *5*, 5414.
- [38] M. Van de Velden, J. Baeyens, A. Brems, B. Janssens, R. Dewil, *Renew. Energy* **2010**, *35*, 232–242.
- [39] E. Ranzi, a Cuoci, T. Faravelli, a Frassoldati, G. Migliavacca, S. Pierucci, S. Sommariva, *Energy and Fuels* **2008**, *22*, 4292–4300.
- [40] D. Mohan, C. U. Pittman, P. H. Steele, *Energy & Fuels* **2006**, *20*, 848–889.
- [41] V. Mamleev, S. Bourbigot, J. Yvon, *J. Anal. Appl. Pyrolysis* **2007**, *80*, 151–165.
- [42] X. Zhou, W. Li, R. Mabon, L. J. Broadbelt, *Energy Technol.* **2017**, *5*, 52–79.
- [43] G. J. Lv, S. B. Wu, R. Lou, *BioResources* **2010**, *5*, 2051–2062.
- [44] Y. Y. Peng, S. B. Wu, *Cellul. Chem. Technol.* **2011**, *45*, 605–612.
- [45] P. F. Britt, A. C. Buchanan, M. J. Cooney, D. R. Martineau, *J. Org. Chem.* **2000**, *65*, 1376–1389.
- [46] C. a. Mullen, A. a. Boateng, *Energy and Fuels* **2008**, *22*, 2104–2109.
- [47] D. J. Nowakowski, A. V. Bridgwater, D. C. Elliott, D. Meier, P. de Wild, *J. Anal. Appl. Pyrolysis* **2010**, *88*, 53–72.
- [48] Y. P. Timilsena, I. G. Audu, S. K. Rakshit, N. Brosse, *Biomass and Bioenergy* **2013**, *52*, 151–158.
- [49] H. Kono, S. Yunoki, T. Shikano, M. Fujiwara, T. Erata, M. Takai, *J. Am. Chem. Soc.* **2002**, *124*, 7506–7511.
- [50] J. Zhang, Y. S. Choi, C. G. Yoo, T. H. Kim, R. C. Brown, B. H. Shanks, *ACS Sustain. Chem. Eng.* **2015**, *3*, 293–301.
- [51] Y. Zhou, H. Stuart-Williams, G. D. Farquhar, C. H. Hocart, *Phytochemistry* **2010**, *71*, 982–993.
- [52] M. Carrier, J. E. Joubert, S. Danje, T. Hugo, J. Görgens, J. H. Knoetze, *Bioresour. Technol.* **2013**, *150*, 129–138.
- [53] K. Papadakis, S. Gu, A. V. Bridgwater, *Chem. Eng. Sci.* **2009**, *64*, 1036–1045.
- [54] C. E. Greenhalf, D. J. Nowakowski, a. B. Harms, J. O. Titiloye, a. V. Bridgwater, *Fuel* **2013**, *108*, 216–230.
- [55] C. a. Mullen, G. D. Strahan, A. a. Boateng, *Energy and Fuels* **2009**, *23*, 2707–2718.
- [56] W. J. DeSisto, N. Hill, S. H. Beis, S. Mukkamala, J. Joseph, C. Baker, T.-H. Ong, E. A. Stemmler, M. C. Wheeler, B. G. Frederick, et al., *Energy & Fuels* **2010**, *24*, 2642–2651.
- [57] L. Ingram, D. Mohan, M. Bricka, P. Steele, D. Strobel, D. Crocker, B. Mitchell, J. Mohammad, K. Cantrell, C. U. Pittman Jr, *Energy & Fuels* **2008**, *22*, 614–625.

FULL PAPER

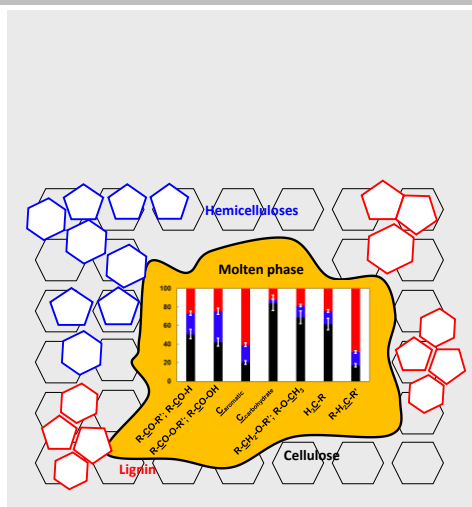
FULL PAPER

Quantitative mapping of functional groups for fast pyrolysis bio-oil.

Marion Carrier,* Michael Windt, Bernhard Ziegler, Jörn Appelt, Bodo Saake, Dietrich Meier and Anthony Bridgwater

Page 1. – Page 12.

Quantitative insights into the Fe Pyrolysis of Extracted Cellulose Hemicelluloses and Lignin



FULL PAPER

Captions for Figures and Schemes

Scheme 1. Potential illustration of lignocellulosic blocks extracted from *Zea Mays*.

Figure 1. Chromatogram (GC-FID) resulting from the pyrolysis of extracted biopolymers from *Zea Mays*: (—) mixture; (—) cellulose; (—) hemicelluloses and (—) lignin.

Figure 2. Mapping of pyrolysis regimes according to heat transport. Adapted from Paulsen *et al.* [33]. Heat-transport map for (■) Pyroprobe; (■) Micro-reactor at ca. 550°C.

Scheme 2. Intra- and extra-particle mass and heat transport events.

Figure 3. Confirmation of the product identity, furfural, and lack of scrambling by comparing experimental and predicted MS fragmentation patterns (Ratio distribution vs mass/charge ratio-m/z) of FP products from mixtures of unlabelled cellulose (Cell-12C), hemicelluloses (Hemi-12C) lignin (Lig-12C) and carbon-13 enriched cellulose (Cell-13C), hemicelluloses (Hemi-13C) and lignin (Lig-13C) – a) Mixtures of Cellulose and Lignin processed in Py-GC/MS; b) and c) Mixtures of Cellulose, Hemicelluloses and Lignin processed respectively in Py-GC/MS and the micro-reactor

Figure 4. Yield of fast pyrolysis products for 550°C. (■) char yield; (□ + □) volatiles yield; (□) total GC-detectable product yield; (□) non-detected products yield obtained by difference.

Figure 5. Relative proportions (%) of the important fractions in bio-oil.

Figure 6. Relative portion (%) of chemical groups within enriched bio-oils based on liquid-state ¹³C-NMR analyses: (■) Cell-¹³C; (■) Hemi-¹³C; (■) Lig-¹³C; (■) MX¹³C; (■) Maize-¹³C.

Figure 7. Carbon source for chemical families according extracted biopolymers: (■) Cellulose; (■) Hemicelluloses; (■) Lignin.

Figure 8. Ratio deviation between experimental and theoretical yields of organic groups for: a) Cellulose; b) Hemicelluloses and c) Lignin.

Tables

Table 1. Ultimate analysis of unlabelled and extracted materials in (wt.%).

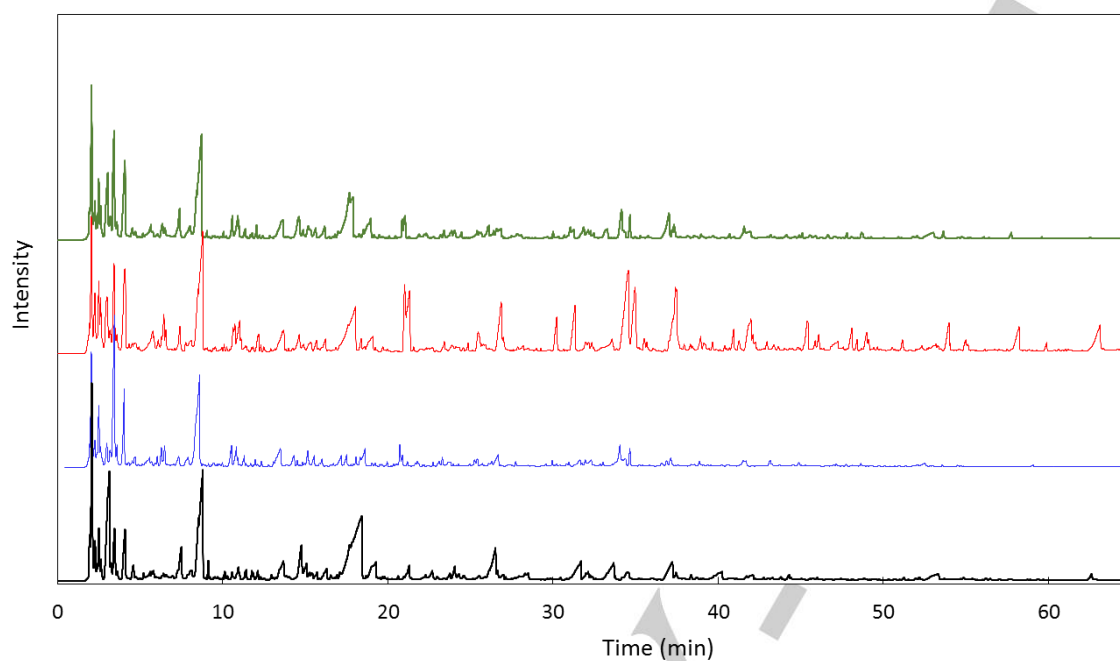
Feedstock	C	H	N	S	O + Ash	H/C
Maize	41.6	5.65	1.31	0.06	51.4	0.14
Cellulose	42.8	6.38	0	0	50.9	0.15
Hemicelluloses	34.6	5.35	0.75	0	59.3	0.16
Lignin	49.9	6.08	1.43	0	42.6	0.12

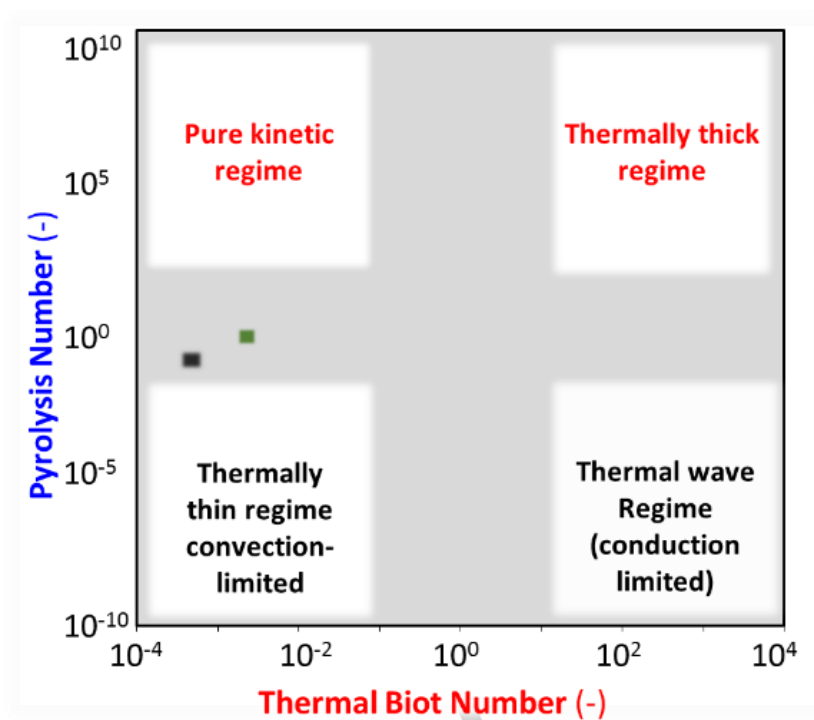
Table 2. General chemical formula.

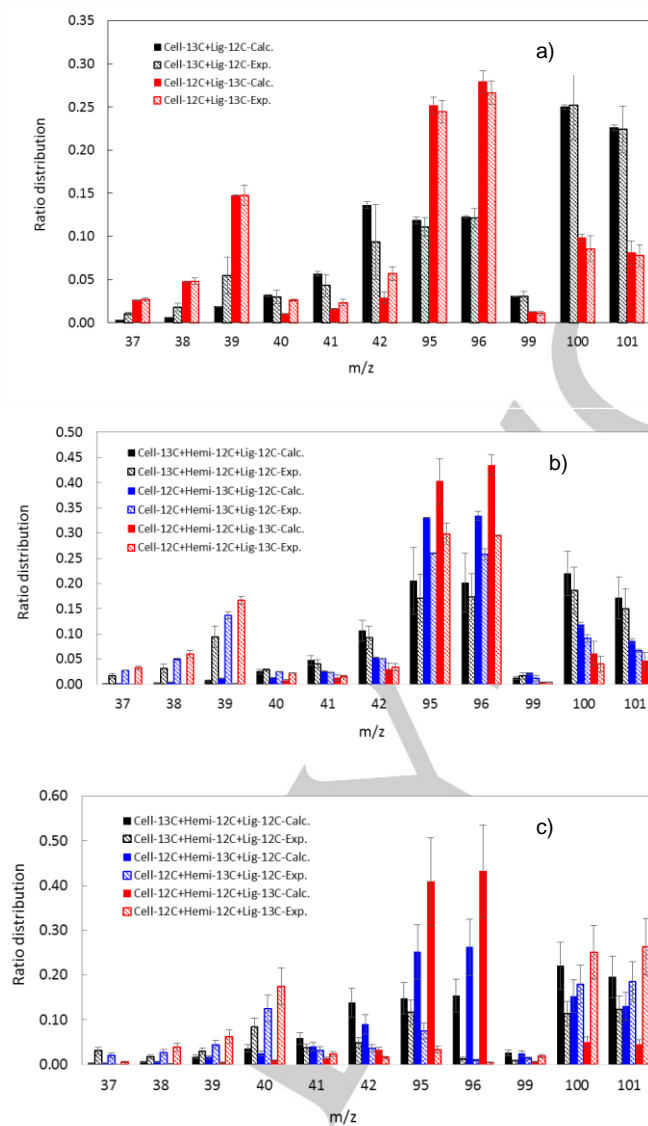
	Cellulose	Hemicelluloses	Lignin
This study	C _{5.6} H ₁₀ O ₅	C ₅ H ₉ O _{6.5}	C ₈ H ₁₁ O ₅
Literature Measured		C _{5.2} H _{9.7} O ₅ ^[28]	C _{10.2} H _{12.2} O _{3.8} N _{0.2} ^[7]
General	(C ₆ H ₁₀ O ₅) _n ^[29]	(C ₅ H ₈ O ₄) _n and (C ₆ H ₁₀ O ₅) _n ^[30]	

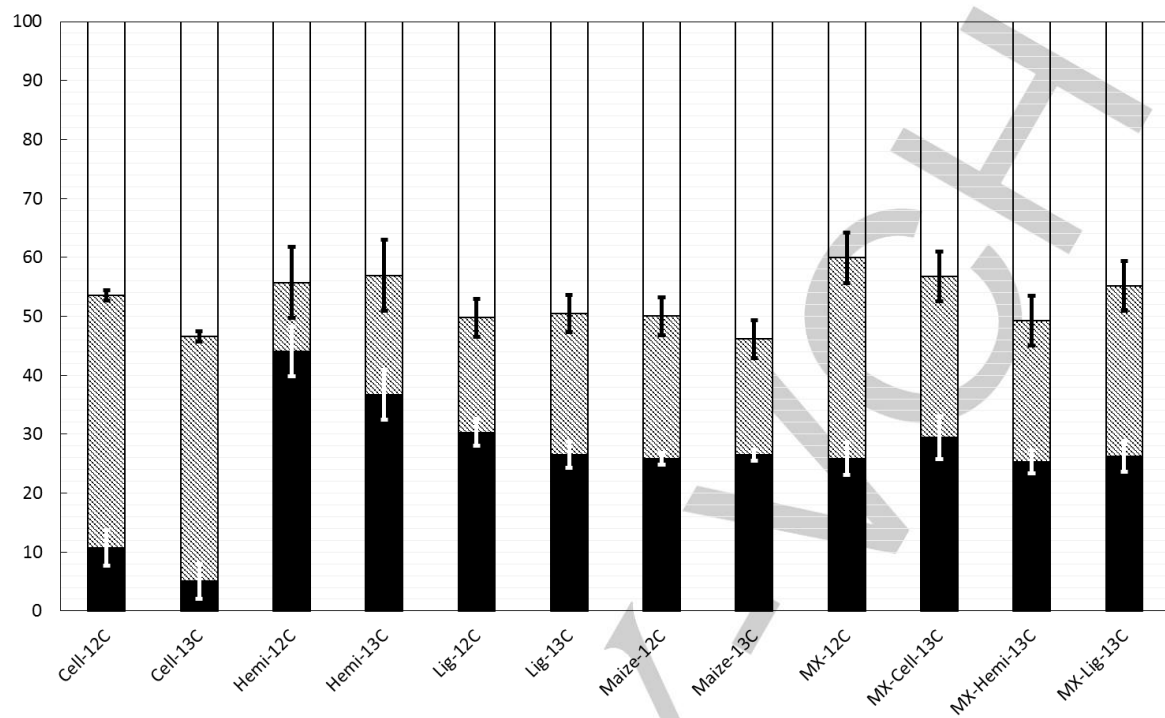
Table 3. Chemical shifts ranges for ¹³C-NMR.

Chemical shift range (ppm)	Groups	Reference
215-180	Ketones, aldehydes	[55]
180-163	Esters, carboxylic acids	[55]
163-110:	Aromatic (general):	[56], [57]
• 125-112	Aromatic compounds (guaiacyl compounds)	
• 112-110	Aromatic compounds (syringyl compounds)	
110-84	Carbohydrate type carbons	
84-54	Methoxy, hydroxyl bond compounds (R- <u>C</u> H ₂ -O-R, R-O- <u>C</u> H ₃)	
54-1:	Primary, secondary, tertiary & quaternary alkyl carbons	
• 34-24	Most of secondary & tertiary alkyl carbons	
• 24-6	Most of primary & some secondary alkyl carbons	

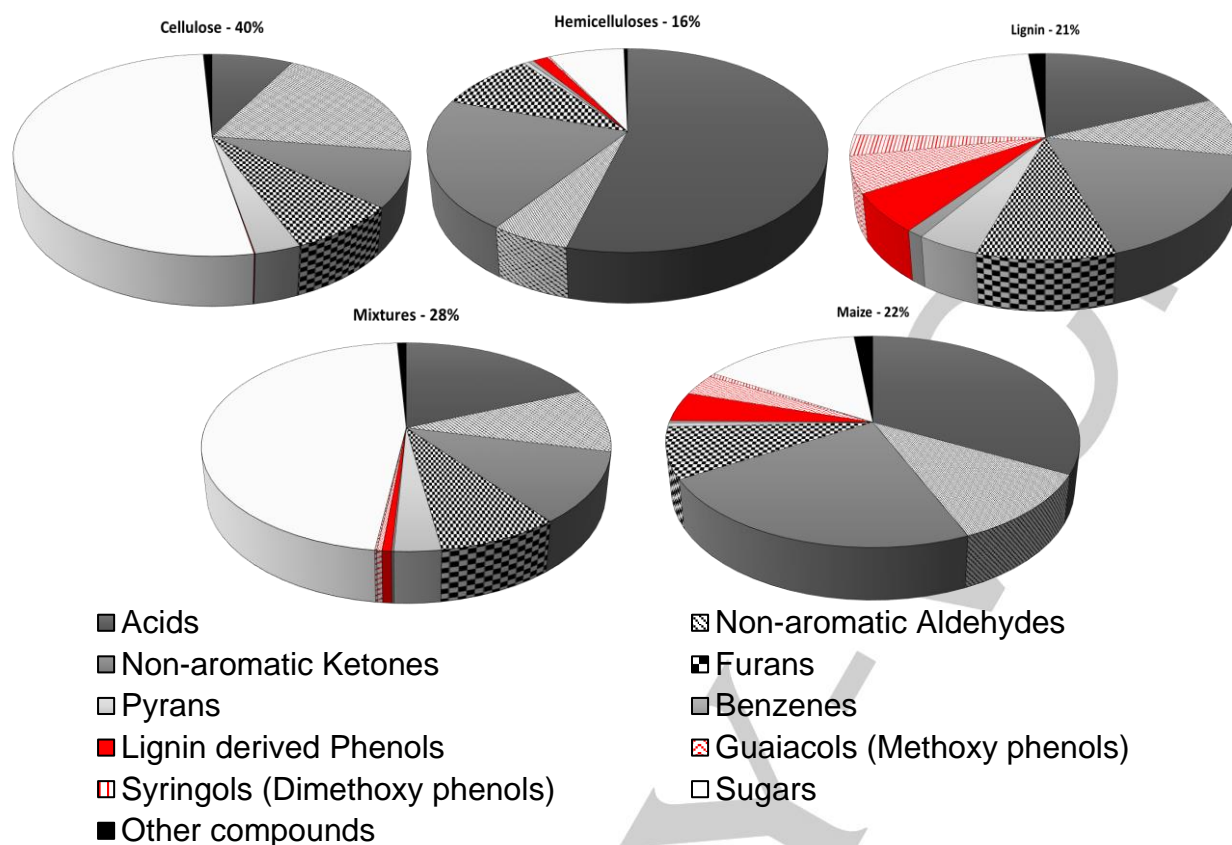


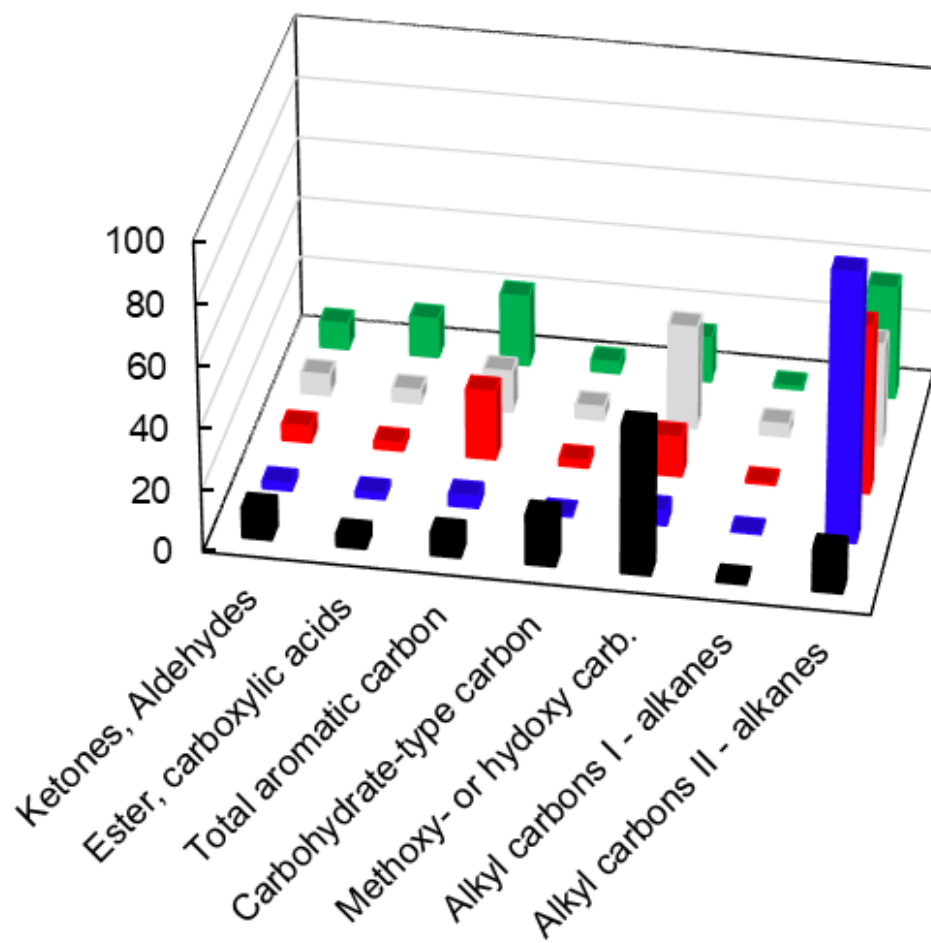






FULL PAPER

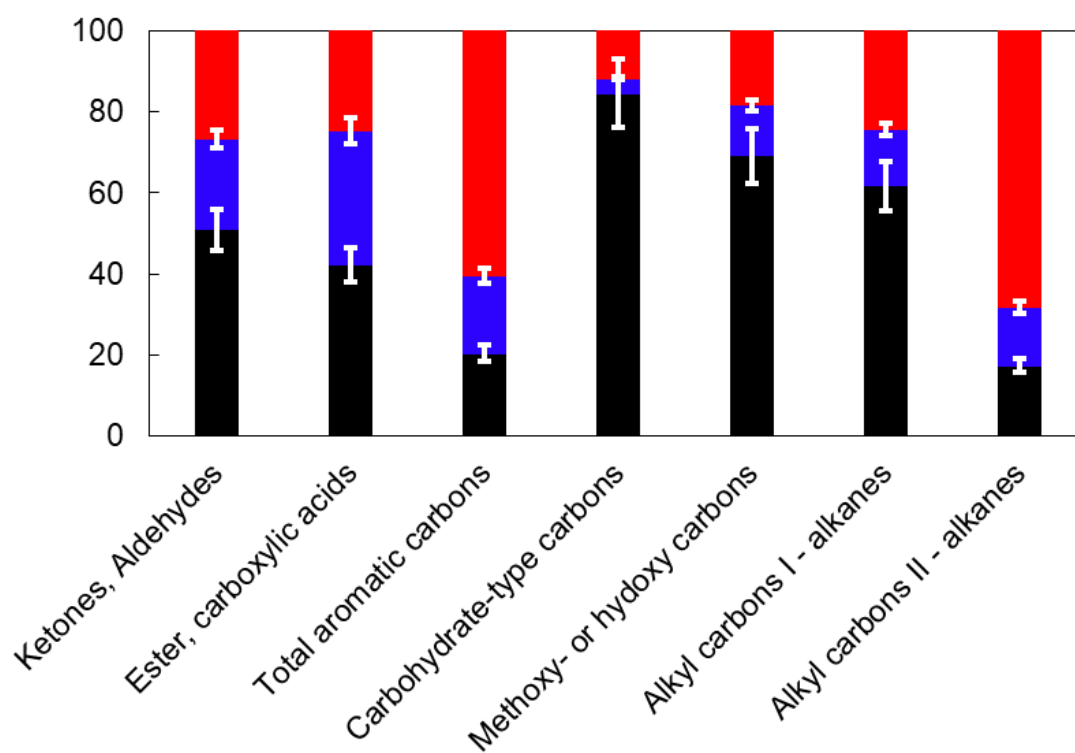




WILEY

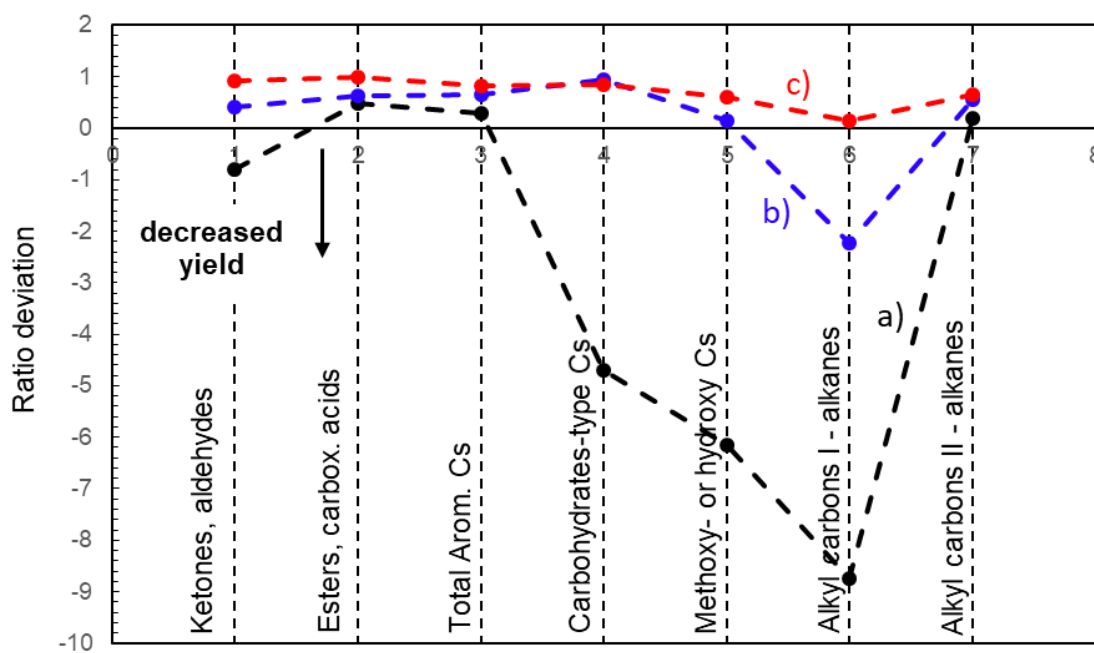
Accepted Manuscript

FULL PAPER



WILEY

Accepted Manuscript



WILEY

Accepted Manuscript

